frontiers in Energy Research

ORIGINAL RESEARCH
published: 12 January 2022
doi: 10.3389/fenrg.2021.784703

Check for updates

RETRACTED: Bi-Level Optimization Dispatch of Integrated-Energy Systems With P2G and Carbon Capture

Zongnan Zhang, Jun Du, Menghan Li, Jing Guo, Zhenyang Xu and Weikang Li*

School of Energy and Power, Jiangsu University of Science and Technology, Zhenjiang, China

The power-to-gas (P2G) technology transforms the unidirectional coupling of power network and natural gas network into bidirectional coupling, and its operational characteristics provide an effective way for wind and solar energy accommodation. The paper proposes a bi-level optimal dispatch model for the integrated energy system with carbon capture system and P2G facility. The upper model is an optimal allocation model for coal-fired units, and the lower model is an economic dispatch model for the integrated energy system. Moreover, the upper model is solved by transforming the model into a mixed-integer linear programming problem and calling CPLEX, and the lower model is a multi-objective planning problem, which is solved by improving the small-habitat particle swarm algorithm. Finally, the simulation is validated by the MATLAB platform, and the results show that the simultaneous consideration of carbon capture system and P2G facility improves the economics of the integrated energy system and the capacity of wind and solar energy accommodation.

Keywords: integrated energy systems, carbon capture system, power to gas (P2G), economic dispatch, wind and solar energy accommodation

RETRACTED

OPEN ACCESS

Edited by:
Zahra Hajabdollahi, University of Glasgow, United Kingdom

Reviewed by:
Rohit Bhakar, Malaviya National Institute of Technology, Jaipur, India
Hongxun Hui, University of Macau, China

****Correspondence:***
Jun Du
dujun9988@163.com

Specialty section:
This article was submitted to Process and Energy Systems Engineering, a section of the journal Frontiers in Energy Research

Received: *28 September 2021*
Accepted: *01 December 2021*
Published: *12 January 2022*

Citation:
Zhang Z, Du J, Li M, Guo J, Xu Z and Li W (2022) Bi-Level Optimization Dispatch of Integrated-Energy Systems With P2G and Carbon Capture. Front. Energy Res. 9:784703. doi: 10.3389/fenrg.2021.784703

1 INTRODUCTION

In recent years, the consumption of natural gas as an important fossil energy source has been growing rapidly worldwide, among which gas turbines account for a large proportion of natural gas consumption (Sun et al., 2015), and gas-fired power generation is expected to grow by 230% by 2030 (Ebel et al., 1996; Correa-Posada and Sanchez-Martin, 2014), with a corresponding rapid increase in the number of installed gas turbines, further deepening the degree of coupling of integrated power-gas energy systems (Yu et al., 2018; Cui et al., 2020).

Renewable energy generation represented by wind and solar energy is highly volatile and intermittent, and wind and solar energy can produce large reductions in the case of limited grid regulation resources (Zhang et al., 2015; Bai et al., 2016a; Cui et al., 2016; Hu et al., 2017), while P2G technology provides a new idea for the accommodation of wind and solar energy (Yang et al., 2016; Lin et al., 2019). The P2G technology can produce synthetic natural gas through chemical reactions, thus realizing the conversion of electricity to natural gas, and further deepening the coupling of the integrated electricity-gas energy system, and realizing the two-way coupling of the two systems together with the gas turbine. The literature (Götz et al., 2016) introduces the principle of P2G technology and analyzes its economics; the literature (Götz et al., 2016) detailing the key technologies for each aspect of P2G and providing a systematic analysis of their costs; the literature (Clegg and Mancarella, 2015) analyzes the impact of P2G technology on the operation of electric-gas integrated energy systems from the perspective of long-term operation, but does not analyze its impact on the

accommodation of wind and solar energy. The electrical energy consumed by P2G can change the load distribution of the system, increase the load value in the low load hours, and reuse the surplus wind and solar energy, thus promoting the accommodation of wind and solar energy. The literature (Guandalini et al., 2015) evaluated the P2G technology from the perspective of improving the dispatchability of wind and solar energy, and proved that P2G can improve the dispatchability of wind and solar energy. In the literature (Wei et al., 2017), a robust stochastic optimization model with a refined P2G model was constructed to achieve economic and reliable operation of the system. The literature (Guandalini et al., 2015) combines P2G and gas turbines to study their effects on system wind abandonment.

Carbon capture power plants are low-carbon power plants that reduce carbon emissions relative to traditional thermal power plants while giving them a deeper peaking depth and good load-following capability, making them a good matching power source for wind and solar energy. With the increasing penetration of wind and solar energy, the low-carbon power provided by carbon capture power plants will play an important role in supporting the safe and stable green operation of the power grid. The literature (Kang et al., 2012) provides a detailed analysis of the development potential, technical characteristics, and realization methods of flexible operation of carbon capture power plants, and establishes a more comprehensive research framework, making an important contribution to the research of carbon capture power plants in China. The literature (Xu and Zeng, 2011) analyzed the energy and mass flows of carbon capture power plants and established a thermodynamic model of carbon capture power plants to optimize their thermal efficiency. The literature (Chen et al., 2010) proposed a comprehensive and flexible operation mode of carbon capture power plant and analyzed its electro-carbon characteristics. The results demonstrated that by combining the split-flow and liquid storage operation modes can effectively expand the operation range and achieve the decoupling of CO_2 capture and absorption. In the literature (Zhang et al., 2018a), an online optimization method based on Lyapunov algorithm is proposed to improve the wind and solar energy accommodation by combining P2G technology. The literature (Yang et al., 2018) analyzed the input-output relationship of the energy flow of the combined carbon capture-electricity-to-gas conversion in order to study its impact on CO_2 reduction. The literature (Lu et al., 2013) constructs a power system operation optimization model considering carbon capture power plants in a low-carbon economy based on the generation-carbon capture coordination characteristics of carbon capture power plants. The literature (Qadir et al., 2015) optimally analyzes the benefits of an SPCC plant located in Australia for different hourly electricity prices, different carbon tax prices, and considering new energy subsidies, and concludes that under flexible operating conditions, SPCC plants can achieve higher operating benefits. The paper (Tan et al., 2009) first proposed the "carbon capture and storage (CCS) total combination curve" pinch point diagram method, which can minimize the impact of carbon capture retrofitting on power plants while meeting the carbon emission constraints of the power industry by constructing a CCS total combination curve. Due to the spatio-temporal disparity between P2G and carbon capture systems, further in-depth study of their synergistic operation strategies is needed.

In this paper, based on the above-mentioned literature, a bi-level optimal dispatch model for the integrated energy system with carbon capture system and P2G facility is developed. The upper model is the optimal allocation model for coal-fired units and the lower model is the economic dispatch model for the integrated energy system. Moreover, the upper model is solved by transforming the model into a mixed-integer linear programming problem and calling CPLEX, while the lower model is a multi-objective planning problem and solved by improving the small-habitat particle swarm algorithm. Finally, a modified 6-bus power system with a 7-node natural gas system and a modified 39-bus power system with a 20-node natural gas system are used as examples to demonstrate the validity and reasonableness of the proposed two-layer model.

RETRACTED

2 SYSTEM DESCRIPTION AND MATHEMATICAL MODELING

2.1 Carbon Capture System

Carbon capture and storage technology is currently the optimal choice for the rapid decarbonization of electricity. By equipping existing thermal power units with carbon capture systems to form carbon capture power plants, the carbon emission intensity of the units can be significantly reduced and the captured greenhouse gases can be transported to safe storage sites (Cui et al., 2021a), thus achieving long-term isolation of CO_2 from the atmosphere. The integrated flexible operation of a carbon capture power plant consists of two parts: flue gas split operation and liquid storage operation (Chen et al., 2012). **Figure 1A** shows a diagram of the integrated flexible operation of a carbon capture plant. The capture process and working principle of the carbon capture power plant are detailed in the literature (Kang et al., 2012).

In **Figure 1A**, the system structure consists of three main parts: absorption, regeneration and compression. Firstly, in the absorption process, the boiler flue gas passes through the bottom of the absorption tower and reacts with the absorption liquid in the reverse direction, so that the CO_2 is absorbed and the absorption liquid is converted from lean liquid to rich liquid; secondly, the rich liquid flows into the regeneration tower through the heat exchanger for heating and regeneration, so that the CO_2 is separated by heat and the rich liquid is converted into lean liquid again. The regenerated absorption solution is cooled by the heat exchanger and re-entered into the absorption tower for recirculation absorption. In this process, the heat provided by the reboiler is mainly obtained by extracting a certain percentage of steam from the power generation side; finally, the compression link: the CO_2 is compressed by a compressor for transportation and storage. In **Figure 1B**, the output power (net output power) of the power plant expressed externally is the total output power minus the energy loss of the carbon capture system, where the carbon capture energy consumption includes fixed losses and operational losses (HE et al., 2018; Yuan et al., 2021).

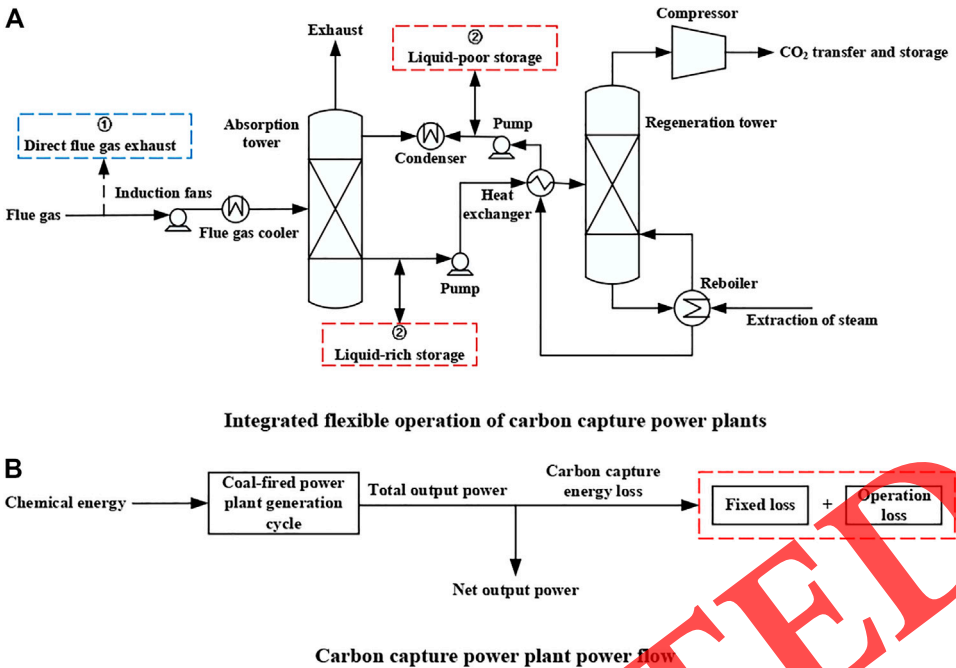

FIGURE 1 | Integrated flexible operation of carbon capture power plants and their power flow. **(A)** Integrated flexible operation of carbon capture power plants **(B)** Carbon capture power plant power flow.

RETRACTED

The flue gas split operation method (shown in **Figure 1A**, ①) adjusts the proportion of direct flue gas exhausted to the atmosphere by controlling the flue gas bypass to achieve flexible adjustment of carbon capture energy consumption and net output power. The liquid storage operation method (shown in **Figure 1A**, ②) makes the rich liquid absorbed from the absorption tower and the rich liquid entering the regeneration tower at the same time no longer equal by introducing a solution memory, i.e., the CO_2 absorption process, which determines the amount of carbon capture, and the solution regeneration process, which determines the energy consumption of carbon capture, are decoupled to a certain extent (Kang et al., 2012).

This integrated and flexible operation approach allows both shifting carbon capture energy consumption that conflicts with load during peak load hours to improve carbon capture levels, and active CO_2 emissions at certain times of the day according to system demand, expanding the net output range of carbon capture plants while increasing dispatch flexibility (Cui et al., 2021b; Cui et al., 2021c).

2.1.1 Mathematical Model of Carbon Capture System

From **Figure 1B**, the net output of the carbon capture plant is the total output minus the energy loss of the carbon capture system (Cui et al., 2021b; Cui et al., 2021c), i.e.

$$\begin{cases} P_{i,t}^{\mathrm{CCG}} = P_{i,t}^{\mathrm{CCN}} + P_{i,t}^{\mathrm{CCL}} \\ P_{i,t}^{\mathrm{CCL}} = P_{i,t}^{\mathrm{CCB}} + P_{i,t}^{\mathrm{CCY}} \end{cases} \tag{1}$$

where $P_{i,t}^{\mathrm{CCG}}$ and $P_{i,t}^{\mathrm{CCN}}$ are the total and net output power of power plant i in time period t; $P_{i,t}^{\mathrm{CCL}}$ is the energy loss of carbon capture system in time period t; $P_{i,t}^{\mathrm{CCB}}$ and $P_{i,t}^{\mathrm{CCY}}$ are the fixed loss and operating loss of carbon capture system in time period t, respectively.

Let the carbon emission intensity of coal-fired power plant i be e_i^{G}, take the value of 0.76. The total CO_2 emissions $E_{i,t}^{\mathrm{CCG}}$ from coal-fired power plant i in time period t can be expressed as

$$E_{i,t}^{\mathrm{CCG}} = e_i^{\mathrm{G}} P_{i,t}^{\mathrm{CCG}} \tag{2}$$

According to **Figure 1A**, the CO_2 capture volume $E_{i,t}^{\mathrm{CO_2}}$ of the carbon capture system is the mass of CO_2 provided by the absorption tower and the solution memory together, i.e.

$$E_{i,t}^{\mathrm{CO_2}} = \beta^{\mathrm{c}} \delta_{i,t} E_{i,t}^{\mathrm{CCG}} + E_{i,t}^{\mathrm{SS}} \tag{3}$$

where β^{c} is the CO_2 capture efficiency, take the value of 0.9; $\delta_{i,t}$ is the flue gas shunt ratio of the flue gas bypass system at time period t; and $E_{i,t}^{\mathrm{SS}}$ is the mass of CO_2 provided by the solution memory at time period t.

At this point, the net CO_2 emissions from the carbon capture plant, i.e., the net carbon de-stocking emissions $E_{i,t}^{\mathrm{CCN}}$, can be expressed as

$$E_{i,t}^{\mathrm{CCN}} = E_{i,t}^{\mathrm{CCG}} - E_{i,t}^{\mathrm{CO_2}} \tag{4}$$

Since the energy loss of the absorption link only accounts for 2–10% of the carbon capture loss, its effect is ignored here. Then the operating loss $P_{i,t}^{\mathrm{CCY}}$ of the carbon capture system can be expressed as

$$\begin{cases} P_{i,t}^{\mathrm{CCY}} = \omega_c E_{i,t}^{\mathrm{CO_2}} \\ \omega_c = \omega_d + \omega_k \end{cases} \tag{5}$$

where ω_c, ω_d, and ω_k are the energy required to capture, regenerate, and compress a unit of CO_2, respectively, the values are all 0.269.

In addition to the above-mentioned operational energy consumption, the carbon capture system also generates some fixed energy consumption $P_{i,t}^{\mathrm{CCB}}$, which is independent of the operational state of the carbon capture system and can be considered as a constant, take the value of 0.76.

The CO_2 extracted from the solution memory exists in the form of compounds in the alcoholamine solution, and the relationship between the mass of CO_2 and the volume of the alcoholamine solution needs to be considered. In this paper, the treatment in the literature (Cui et al., 2021a) converts the mass $E_{i,t}^{\mathrm{SS}}$ of CO_2 that can be extracted from the solution memory into the form of the solution volume $V_{i,t}^{\mathrm{SS}}$, i.e.

$$V_{i,t}^{\mathrm{SS}} = \frac{E_{i,t}^{\mathrm{SS}} M_{\mathrm{MEA}}}{\theta \mu_{\mathrm{L}} \sigma_{\mathrm{L}} M_{\mathrm{CO_2}}} \tag{6}$$

where θ is the regeneration volume of regeneration tower, take the value of 0.3; μ_{L} is the solution concentration, take the value of 30%; σ_{L} is the solution density, take the value of 1.01; $M_{\mathrm{CO_2}}$ is the mass molar mass of CO_2, take the value of 44; M_{MEA} is the molar mass of ethanolamine, take the value of 61.08.

The operational constraints of a carbon capture power plant can be expressed as

$$\begin{cases} 0 \le E_{i,t}^{\mathrm{CO_2}} \le \xi \beta^{\mathrm{c}} \mathrm{e}_i^{\mathrm{G}} P_i^{\mathrm{CCG,max}} \\ -\beta^{\mathrm{c}} \mathrm{e}_i^{\mathrm{G}} \delta_{i,t} P_{i,t}^{\mathrm{CCG}} \le E_{i,t}^{\mathrm{SS}} \\ E_{i,t}^{\mathrm{SS}} \le \xi \beta^{\mathrm{c}} \mathrm{e}_i^{\mathrm{G}} P_i^{\mathrm{CCG,max}} \\ -\beta^{\mathrm{c}} \mathrm{e}_i^{\mathrm{G}} \delta_{i,t} P_{i,t}^{\mathrm{CCG}} \\ 0 \le \delta_{i,t} \le 1 \\ V_{i,T}^{\mathrm{CCF}} = V_{i,0}^{\mathrm{CCF}} + \sum_{t=1}^{T} \left(V_{i,t}^{\mathrm{CCF}} - V_{i,t}^{\mathrm{CCP}} \right) \\ V_{i,T}^{\mathrm{CCP}} = V_{i,0}^{\mathrm{CCP}} + \sum_{t=1}^{T} \left(V_{i,t}^{\mathrm{CCP}} - V_{i,t}^{\mathrm{CCF}} \right) \end{cases} \tag{7}$$

where ξ is the maximum operating condition factor of the resolving tower, take the value of 120; $P_i^{\mathrm{CCG,max}}$ is the maximum power output of the power plant; $V_{i,t}^{\mathrm{CCF}}$ is the volume of solution flowing into the rich liquid storage unit, which is approximately equal to the volume of solution flowing out from the poor liquid storage unit; $V_{i,t}^{\mathrm{CCP}}$ is the volume of solution flowing into the poor liquid storage unit, which is approximately equal to the volume of solution flowing out of the rich liquid storage unit; $V_{i,0}^{\mathrm{CCF}}$ and $V_{i,0}^{\mathrm{CCP}}$ are the initial volumes of the rich liquid and poor liquid storage units, respectively, the values are all 30,000.

In addition, the upper and lower output constraints, minimum start-stop time constraints, and creep constraints for carbon capture power plants are similar to those described below for coal-fired units and are not repeated here.

2.2 Natural Gas System

The natural gas system mainly consists of gas wells, pipelines, compressors, storage equipment and loads, and the corresponding system structure can be briefly depicted in **Figure 2**.

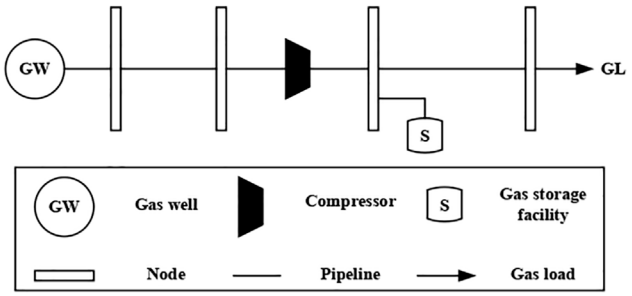

FIGURE 2 | Natural gas system.

2.2.1 Natural Gas System Steady State Model

As can be seen from **Figure 2**, gas wells are the main source of natural gas production, and the constraint on the supply of natural gas $S_{i,t}$ at moment t from a gas well located at node i in the network can be expressed as

$$S_{i,\min} \le S_{i,t} \le S_{i,\max} \tag{8}$$

where $S_{i,\min}$ and $S_{i,\max}$ are the minimum and maximum values of natural gas supply from gas wells located at node i in the network, respectively.

The natural gas load includes residential load, commercial load and industrial load, etc., among which the natural gas load consumed by gas-fired power plants for power generation accounts for a relatively large share. As a coupling node of the power-gas system, the gas consumption of gas power plants depends on the power generation capacity. Since there is an upper and lower bound constraint on the power generation capacity of the unit, the gas load consumed by the gas power plant at node i in the gas network at time t should also have an upper and lower bound constraint, which can be expressed as (Zhang et al., 2018b)

$$GL_{\min} \le GL_{i,\mathrm{gas},t} \le GL_{\max} \tag{9}$$

where $GL_{\min}$ and $GL_{\max}$ are the minimum and maximum values of the gas load consumed by the gas plant at node i in the natural gas network, respectively.

The flow loss of natural gas in the transmission process is similar to the voltage loss of the power system (Barry and Menon, 2005; Tomasgard et al., 2007), there are nodal pressure losses at both ends of natural gas pipelines, and its flow always flows from the high pressure node to the low pressure node. The natural gas pipeline flow rate is determined by the length and diameter of the pipeline, the operating temperature and the pressure at both ends of the pipeline. For a given pipeline, the flow rate as a function of nodal pressure at both ends can be expressed by the Weymouth equation (Li et al., 2017), described as follows.

$$\begin{cases} F_{ij} = sgn(\pi_i, \pi_j) \times C_{ij} \sqrt{\left| \pi_i^2 - \pi_j^2 \right|} \\ sgn(\pi_i, \pi_j) = \begin{cases} 1, & \pi_i \ge \pi_j \\ -1, & \pi_i < \pi_j \end{cases} \end{cases} \tag{10}$$

RETRACTED

$$\pi_i \le \pi_i \le \bar{\pi}_i \tag{11}$$

where F_{ij} is the pipeline flow rate; C_{ij} is the pipeline constant related to temperature, length, diameter, friction, etc.; π is the natural gas pipeline nodal pressure; $sgn(\pi_i, \pi_j)$ is a symbolic function indicating the natural gas flow direction, and its value is 1 when the pressure at node i is greater than the pressure at node j, and -1 vice versa. in **Eq. 11**, the nodal pressure should be within the given operating constraint.

In practice, for non-ring natural gas networks, the correlation matrix between the injected flow at each node and the pipeline flow can be established by the forward back substitution method, similar to the concept of generation transfer factor GSF_e in the DC tide method for power systems, and the natural gas flow transfer factor matrix GSF_{gas} defined to reflect the natural gas supply at each node and the relationship between the load volume and the pipeline flow (Zhang et al., 2018b):

$$F_{ij} = \sum_{m=1}^{NG} GSF_{\text{gas},m,ij} \times (S_m - GL_m) \tag{12}$$

Based on the GSF_{gas} matrix, a link is established between each pipeline flow rate and the nodal injection and outflow gas volumes, thus replacing the nodal flow balance equation. After obtaining the flow rate of each pipeline, the pressure of each node can be calculated according to **Eq. 10**.

As the transmission distance increases, the pressure loss between nodes leads to low pressure at the end nodes, thus limiting the network transmission capacity, so a certain number of booster stations are required to increase the transmission capacity. The most important part of a booster station is a compressor that increases the pressure of natural gas, which can raise the pressure at the nodes, but consumes energy. To some extent, a booster station can be equated to a special transformer: a fixed pressure or a fixed ratio while consuming energy. In this paper, the booster station is modeled as a fixed ratio, and the energy consumed is derived from electrical energy, contained in the load of the grid node where it is located (Bai et al., 2016b), which can be expressed as follows (Zhang et al., 2018b):

$$H_{\text{com}} = BF_{ij}\left[\left(\frac{\pi_i}{\pi_j}\right)^Z - 1\right] \tag{13}$$

$$P_{\text{com}} = H_{\text{com}}\left(0.7479 \times 10^{-5}\right) \tag{14}$$

where H_{com} is the power required by the compressor; F_{ij} is the flow rate through the compressor; B and Z are constants; and P_{com} is the electrical load of the electrically driven compressor.

2.2.2 Coupling With Power System

The main coupling parts of the power system and the natural gas system are the gas turbine and the P2G. The gas turbine and the P2G realize the bi-directional coupling of the power system and the natural gas system.

(1) Gas turbine: For power systems, the gas turbine is a resource on the energy supply side, while in natural gas systems it is a load. The consumption characteristics of the gas turbine operation can be expressed as:

$$Q_{MT} = \frac{P_{MT}^t \Delta t}{\eta_e LHV_f} \tag{15}$$

where P_{MT}^t is the power of the gas turbine at time t; Δt is the gas turbine operating time; η_e is the gas turbine power generation efficiency, take the value of 32%; LHV_f is the low-level calorific value of natural gas, take the value of 9.7; and Q_{MT} is the amount of natural gas consumed by the gas turbine during the operating time.

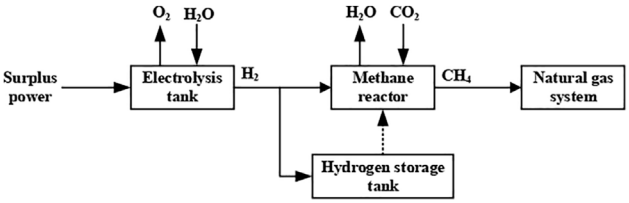

FIGURE 3 | P2G two-stage operation.

(2) P2G: The power-to-gas technology consists of two processes (Clegg and Mancarella, 2015): electric hydrogen production and hydrogen methanation. Hydrogen and oxygen are generated by electrolysis of water by passing high intensity direct current through an electrolyzer. Part of the generated hydrogen is reacted with carbon dioxide in a methane reactor by Sabatier reaction to form methane and water, and the other part is stored in a hydrogen storage tank and supplied to the methane reactor when needed. The produced methane is injected directly into the natural gas network to supply the gas load or other gas units. **Figure 3** gives an illustration of the two-stage operation principle of the power-to-gas conversion. Among them, the surplus power in the figure mainly comes from the excess power generated by the wind and light abandonment periods.

For the use of P2G, a new model of flexibility metric based on redundant line packets and gas storage was proposed in the literature (Liu et al., 2021). Simulation results show that P2G not only facilitates the operation of integrated energy systems, but also has better economics. In the literature (Du et al., 2017), a microgrid optimization model was developed using system cost minimization as the objective function and taking into account the interests of both supply and demand, including technologies such as P2G. The test results show that considering P2G technology, the frequently used plug-in hybrid vehicles can effectively reduce the system operation cost and improve the utilization of renewable energy by working in concert with renewable energy in different scenarios. In this paper, P2G converts surplus electricity to natural gas, which can effectively reduce the gas purchase cost of gas turbines because wind and solar energy can be the main source of surplus energy, and energy sources such as energy storage batteries are only supplementary,

RETRACTED

and the increase of their electricity production cost is less. In addition, P2G's accommodation of wind and solar energy reduces the impact on the power system caused by fluctuations in wind and solar energy. And the CO_2 emitted during the operation of coal-fired units serves as an important source of CO_2 for P2G, reducing the pollution of the system to the environment. Combined with the above, P2G has high feasibility and economy to convert surplus electricity to natural gas.

Combined with the above P2G facility operation process, the corresponding operation model is constructed as follows.

In an electrolysis plant, the hydrogen $Q_{p2g}^{H_2}$ produced by electrolysis of water can be expressed as

$$Q_{p2g}^{H_2} = \frac{P_{p2g}^{in}\eta_{p2g}^{H_2}\xi_{e,g}}{HHV_{H_2}} \tag{16}$$

where P_{p2g}^{in} is the input power of the P2G facility; $\eta_{p2g}^{H_2}$ is the efficiency of electric hydrogen production in the P2G facility, take the value of 73%; $\xi_{e,g}$ is the coefficient of conversion of electric energy to equivalent heat energy, take the value of 3.41; and is the high calorific value of hydrogen, take the value of 0.342.

Where the hydrogen produced by electrolysis of water is injected into the methane reactor as $Q_{CH_4}^{H_2,in}$ and the hydrogen injected into the hydrogen storage tank as $Q_s^{H_2,in}$. Then we have

$$Q_{p2g}^{H_2} = Q_{CH_4}^{H_2,in} + Q_s^{H_2,in} \tag{17}$$

The input power of electrolytic devices is usually limited to a certain range (Lin et al., 2017).

$$I_{p2g}^{in}P_{p2g,min}^{in} \le P_{p2g}^{in} \le I_{p2g}^{in}P_{p2g,max}^{in} \tag{18}$$

where $P_{p2g,min}^{in}$ and $P_{p2g,max}^{in}$ are the minimum and maximum input power of the electrolysis equipment in the P2G facility; I_{p2g}^{in} is the operating state of the electrolysis equipment in the P2G facility.

The hydrogen storage tank needs to satisfy the hydrogen storage balance constraint, the hydrogen storage size constraint, the injected hydrogen flow size constraint and the removed hydrogen flow size constraint during the operation (Wei et al., 2017).

$$E_{st}^{H_2} = E_{s,t-1}^{H_2} + (Q_{st}^{H_2,in} - Q_{st}^{H_2,out})\Delta t \tag{19}$$

$$E_{s,min}^{H_2} \le E_{st}^{H_2} \le E_{s,max}^{H_2} \tag{20}$$

$$0 \le Q_{st}^{H_2,out} \le Q_{s,max}^{H_2,out} \tag{21}$$

$$0 \le Q_{st}^{H_2,in} \le Q_{s,max}^{H_2,in} \tag{22}$$

where $E_{st}^{H_2}$ and $E_{s,t-1}^{H_2}$ are the hydrogen storage capacity of the hydrogen storage tank in time period t and t-1, respectively; $Q_{st}^{H_2,in}$ and $Q_{st}^{H_2,out}$ are the hydrogen flow rates injected and removed from the hydrogen storage tank in time period t, respectively; Δt is a single operating time period; $E_{s,min}^{H_2}$ and $E_{s,max}^{H_2}$ are the minimum hydrogen storage capacity and capacity of the hydrogen storage tank, respectively; $Q_{s,max}^{H_2,in}$ and $Q_{s,max}^{H_2,out}$ are the maximum injection and removal flow rates of the hydrogen storage tank, respectively.

In a methanation plant, the CO_2 consumed and the methane synthesized can be expressed separately as

$$Q_{p2g}^{CO_2} = Q_{CH_4,s}^{H_2,in} \cdot \phi_{H_2-CO_2} \tag{23}$$

$$Q_{p2g}^{CH_4} = Q_{CH_4,s}^{H_2,in} \cdot \phi_{H_2-CH_4} \tag{24}$$

where $Q_{p2g}^{CO_2}$ and $Q_{p2g}^{CH_4}$ are the amount of CO_2 consumed by the Sabatier reaction and the amount of methane synthesized in the P2G facility, respectively; $\phi_{H_2-CO_2}$ and $\phi_{H_2-CH_4}$ are the reaction coefficients between H_2 and CO_2 and between H_2 and CH_4 in the Sabatier reaction, respectively, the values are all 0.25; $Q_{CH_4,s}^{H_2,in}$ is the sum of the hydrogen produced by electrolysis of water injected into the methane reactor and the hydrogen stored in the hydrogen storage tank injected into the methane reactor.

It is worth stating that carbon capture power plants are formed by equipping existing fossil fuel power plants with carbon capture systems, which capture carbon dioxide from the flue gas of fossil fuel power plants. P2G consists of two processes: electric hydrogen production and hydrogen methanation: electrolysis of water: $2H_2O \rightarrow 2H_2 + O_2$ and methane synthesis: $CO_2 + 4H_2 \rightarrow CH_4 + 2H_2O$, while the carbon dioxide required for the hydrogen methanation process in the P2G plant is provided by the carbon dioxide captured by the carbon capture system. The methane produced by the P2G plant is injected directly into the natural gas system to supply the gas load or other gas units.

3 BI-LEVEL OPTIMAL DISPATCHING MODEL WITH CARBON CAPTURE AND P2G

The structure of the integrated energy system used in this paper and the framework of the constructed bi-level optimal dispatching model are shown in **Figure 4** (Zhang et al., 2018b). The upper model of the proposed bi-level model is the optimal allocation model of thermal power units, and the lower model is the economic dispatch model of the integrated energy system. It is worth stating that the P2G technology constitutes a bi-directional coupled electricity-gas integrated energy system in the power system with important significance: converting excess power generation from renewable energy into natural gas for utilization or storage, reducing the impact of renewable energy on the power grid and improving the smoothness of the power system input; converting surplus energy from conventional power generation equipment in the power system during the low load period into natural gas and releasing it during the load The conversion of surplus energy from conventional power generation equipment to natural gas during low load periods and its release through gas turbines and other equipment during high load periods reduces the gap between peak and valley system output and improves the smoothness of system output; the ability to consume carbon dioxide through carbon capture in P2G plants and stations improves the low-carbon nature of the system.

3.1 Optimal Allocation Model for Coal-Fired Units

The optimal allocation of coal-fired units is an important part of the economic dispatch plan before the day, including the determination of unit start/stop status and economic load allocation. Since the start-stop status and economic load allocation are interdependent, in

RETRACTED

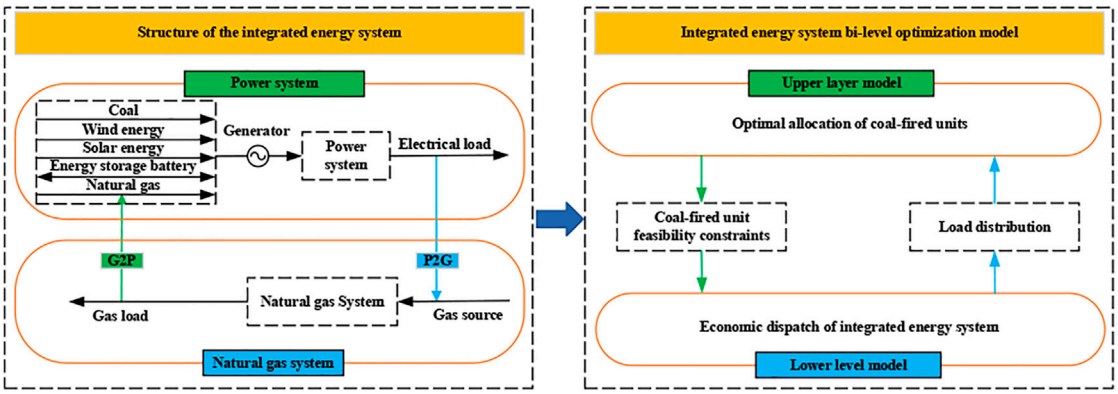

FIGURE 4 | Integrated energy system architecture and bi-level modeling framework. Optimal allocation model for coal-fired units.

order to obtain the best optimization effect, the two cannot be simply decoupled and the joint optimization method is used to achieve the optimal allocation of coal-fired units. The joint optimization method is a direct model of unit combination with the objective of minimizing costs, considering multiple constraints and combining equal micro-increment rates for day-ahead economic dispatch.

With the generation cost of the unit and the start-stop cost of the unit as the target, and each unit must also meet certain constraints, the unit combination model of the day-ahead economic dispatch is established, and the joint optimization of determining the start-stop status of the unit and the economic load distribution is realized by solving a more complete unit combination model. The specific model can be expressed as follows:

Objective function:

$$\begin{cases} \min F\left(P_i^t\right) = \sum_{t\in\Omega_T}\sum_{i\in\Omega_{CU}}\left[F_i\left(P_i^t\right)u_i^t + \right. \\ \left. F_{si}\left(t\right)u_i^t\left(1-u_i^{t-1}\right)\right] \\ F_i\left(P_i^t\right) = \alpha_i\left(P_i^t\right)^2 + \beta_i P_i^t + \gamma_i \\ F_{si}\left(t\right) = \xi_i + \phi_i\left[1-\exp\left(\frac{q_i^t}{\tau_i}\right)\right] \end{cases} \tag{25}$$

Constraints:

$$\begin{cases} u_i^t = 0 or 1 \\ \sum_{i\in\Omega_{CU}} u_i^t P_i^t = P_{\mathrm{D}}^t \\ \sum_{i\in\Omega_{CU}} u_i^t P_{i,\max} - P_{\mathrm{D}}^t \geqslant R^t \\ u_i^t P_{i,\min} \leqslant P_i^t \leqslant u_i^t P_{i,\max} \\ \left(u_i^t - u_i^{t-1}\right)\left(w_i^{t-1} - w_i^{\min}\right) \leqslant 0 \\ w_i^t = u_i^t\left(w_i^{t-1}+1\right) \\ \left(u_i^t - u_i^{t-1}\right)\left(q_i^{t-1} - q_i^{\min}\right) \leqslant 0 \\ q_i^t = \left(1-u_i^t\right)\left(q_i^{t-1}+1\right) \\ P_{i,down} \leqslant u_i^t P_i^t - u_i^{t-1}P_i^{t-1} \leqslant P_{i,up} \\ -P_{k,\max} \leqslant \sum_{j=1}^{n} S_{j,k}P_{j,\mathrm{net}} \leqslant P_{k,\max} \\ i \in \Omega_{CU} \\ t \in \Omega_T \end{cases} \tag{26}$$

where Ω_T and Ω_{CU} are the dispatching time period and the set of coal-fired units, respectively; P_i^t is the output of unit i at time t; $F_i(P_i^t)$ is the generation cost function of unit i; u_i^t is the operating status of unit i at time t; $F_{si}(t)$ is the start-up and shutdown cost function of unit i; α_i, β_i and γ_i are the generation cost coefficients of unit i; ξ_i is the fixed cost of start-up and shutdown of unit i; ϕ_i and τ_i are the correlation coefficients of unit i; q_i^t is the time that unit i has been in continuous operation in time period t; $q_i^{\min}$ is the minimum continuous start-up time allowed for unit i; P_{D}^t is the load at time t; $P_{i,\max}$ and $P_{i,\min}$ are the maximum and minimum output of unit i, respectively; R^t is the standby capacity at time t; w_i^t is the time unit i has been continuously offline at time t; $w_i^{\min}$ is the minimum continuous offline time allowed for unit i; $P_{i,up}$ and $P_{i,down}$ are the lift-off and lift-out rates of unit i, respectively; $P_{k,\max}$ is the stability limit of line k; $S_{j,k}$ is the sensitivity of injected power of bus j to power flow of line k; $P_{j,\mathrm{net}}$ is the net injected power at bus j.

3.2 Integrated Energy System Economic Dispatch Model

The economic dispatch model of integrated energy system established in this paper is a dual-objective model, with objective one being the operating cost and objective two being the environmental cost. The operating cost consists of the cost of power generation and start-stop cost of coal-fired units, the operating cost of gas turbines, the operating and maintenance cost of energy storage batteries, the gas production cost of natural gas wells and the penalty cost of scenery abandonment. The environmental cost is composed of two parts: the carbon tax cost of carbon dioxide emission from fossil fuel units and the carbon dioxide transmission and storage cost of carbon capture units. As for the constraints, such as unit climbing constraints, power balance and other constraints, they are not repeated here, but only added. The specific model can be expressed as follows.

RETRACTED

Operating cost objective function:

$$\begin{cases} \min\left(F_1+F_2+F_3+F_4+F_5\right) \\ F_1 = F\left(P_i^t\right) \\ F_2 = \sum\limits_{t\in\Omega_T}\sum\limits_{MT\in\Omega_{GM}} \rho_{MT} Q_{MT}^t \\ F_3 = \sum\limits_{t\in\Omega_T}\sum\limits_{j\in\Omega_{GO}} K_{om,j} P_j^t \\ F_4 = \sum\limits_{t\in\Omega_T}\sum\limits_{gas\in\Omega_{GG}} \rho_{gas} Q_{gas}^t \\ F_5 = \sum\limits_{t\in\Delta_T}\left(\begin{array}{c}\sum\limits_{w\in\Omega_{GW}} \phi_w^t c_w^t \Delta P_w^t + \\ \sum\limits_{pv\in\Omega_{GP}} \phi_{pv}^t c_{pv}^t \Delta P_{pv}^t\end{array}\right) \\ \phi_{w/pv}^t = 1+\dfrac{\Delta P_{w/pv}^t}{\bar{P}_{w/pv}^t} = 1+\dfrac{\bar{P}_{w/pv}^t - P_{w/pv}^t}{\bar{P}_{w/pv}^t} \end{cases} \tag{27}$$

Environmental cost objective function:

$$\min \sum_{t\in\Omega_T}\left\{\begin{array}{c}\rho_c^t\left(\sum\limits_{i\in\Omega_{FU}} \mu_i P_i - \sum\limits_{c\in\Omega_{CCU}} Q_c^t\right)+ \\ \rho_s^t \sum\limits_{c\in\Omega_{CCU}} Q_c^t\end{array}\right\} \tag{28}$$

Constraints:

$$\begin{cases} P_w^t \le P_w^t \le \bar{P}_w^t \\ P_{pv}^t \le P_{pv}^t \le \bar{P}_{pv}^t \\ SOC_{\min} \leqslant SOC_t \leqslant SOC_{\max} \\ SOC_t = SOC_0 + \dfrac{\sum\limits_{t\in\Omega_T} P_{bat}^t \Delta t}{C_N} \end{cases} \tag{29}$$

Where Ω_{GM}, Ω_{GO}, Ω_{GG}, Ω_{GW}, Ω_{GP}, Ω_{FU}, Ω_{CCU} are the set of gas turbines, the set of energy storage cells, the set of gas wells for natural gas, the set of wind farms, the set of photovoltaic power farms, the set of fossil fuel units and the set of carbon capture units, respectively; ρ_{MT}, ρ_{gas}, ρ_c^t, ρ_s^t are the fuel price of gas turbines, the unit gas production cost of gas wells, the carbon tax price and the unit carbon dioxide price of transmission and storage, respectively; $K_{om,j}$ is the energy storage cell j's operation and maintenance cost factor, take the value of 0.84; Q_{gas}^t is the natural gas supplied by the natural gas well at moment t; $c_{w/pv}^t$ is the barrier factor for wind and solar energy, respectively; $c_{w/pv}^t$ is the abandonment penalty cost factor for wind and solar energy, respectively; $\Delta P_{w/pv}^t$ is the abandoned power for wind and solar energy at moment t, respectively; $P_{w/pv}^t$ is the forecasted output of wind and solar energy at moment t, respectively; $\bar{P}_{w/pv}^t$ is the forecasted maximum possible output of wind and solar energy at moment t, respectively; $\underline{P}_{w/pv}^t$ is the predicted minimum possible output of wind and solar energy at moment t, respectively; μ_i is the carbon dioxide emission intensity of fossil fuel units; P_i is the total power generated by fossil fuel units; Q_c^t is the carbon dioxide handled by carbon capture units at moment t; SOC_0 and SOC_0 are the charge states of energy storage batteries at moment t and the initial charge state, respectively; $SOC_{\min}$ and $SOC_{\max}$ are the minimum and maximum values of charge states of energy storage batteries, respectively; P_{bat}^t is the charge and discharge power of energy storage batteries at moment t; is the nominal capacity of the energy storage battery.

4 SOLUTION OF BI-LEVEL MODEL

4.1 Solution of the Upper Model

From the above modeling process, it can be seen that the constructed optimal allocation model for coal-fired units is a mixed integer nonlinear programming problem, and it is difficult to obtain the global optimal solution by traditional mathematical methods. Therefore, in this paper, the nonlinear equations are linearized by segments, and the constructed model is converted into a mixed integer linear programming problem, and the YALMIP modeling toolkit embedded in MATLAB software is used to realize the program writing, and then the CPLEX solver is called to solve the model. The specific solving steps are as follows:

Step 1: Input parameters;
Step 2: Writing objective functions and constraints;
Step 3: Calling the CPLEX solver;
Step 4: Get optimized results.

Among them, the input parameters include relevant parameters of coal-fired units; relevant parameters of carbon capture systems; and relevant parameters of power load, wind and solar energy forecasts. The objective function and constraints have been given in **Section 3.1**.

4.2 Solution of the Lower Model

The integrated energy system optimization problem is a nonlinear optimization problem with complex constraints and high solution dimensionality (Zhang et al., 2017). In this paper, an improved small-habitat particle swarm algorithm is used to solve the problem.

The particle swarm algorithm originated from the study of the foraging behavior of birds (Kennedy and Eberhart, 1995), and the core idea can be understood as follows: the solution process of each optimization problem is imagined as a particle search process in D-dimensional space, and each particle corresponds to a fitness value, which is determined by each objective function, and in the search process, each particle corresponds to a different flight direction and flight distance due to its own flight speed, and in the whole flight During the search process, each particle is constantly approaching the search direction of the optimal particle, so as to approach the optimal solution. It can be seen that the complex global search process of particle swarm algorithm is composed of many interacting local searches. With this strategy, the particle swarm algorithm is able to solve high-dimensional, constrained complex problems, but the local search capability is too prominent, causing problems

RETRACTED

such as premature convergence and easy to fall into local extremes (Chang et al., 2021).

The microhabitat technique is derived from the theory of evolution in nature, in which there is a group of species with similar living habits in a specific environment, and these species need to communicate and compete in this environment, which is called microhabitat. Species with strong survival ability stay in the microhabitat, while those with weak survival ability are eliminated, and under this mechanism of "survival of the fittest," species in the microhabitat evolve. Using the microhabitat technique, each generation of individuals is divided into several classes, and a number of individuals with greater adaptability in each class are selected as the best representatives of a class to form a swarm, which dynamically forms a relatively independent search space to achieve simultaneous search of multiple extremal regions, in order to overcome the defects of early convergence and easy to fall into local optimum of the basic particle swarm algorithm, and obtain better recognition accuracy and convergence speed (Lu and Li, 2019; Rani and Mahapatra, 2019). Thus, this paper adopts the improved small habitat particle swarm algorithm with high reasonableness and feasibility.

In the particle swarm algorithm based on the small habitat technique, the division of the whole population is crucial. Since most of the applications of the small habitat technique in the current particle swarm algorithm draw on the previous empirical values of the small habitat radius, it has some limitations, for which a method to solve the small habitat radius is proposed in this paper, as shown in **Eq. 30**. Initialize the particle swarm, find one particle X_i randomly as the extreme point of individual history memory, and then calculate the minimum Euclidean distance d_i between other ordinary particles X_j and particle X_i. Then its average value is the radius σ_{share} of this small habitat. Particles whose minimum Euclidean distance from particle X_i is less than or equal to the small habitat radius σ_{share} belong to this small habitat particle group X_p, and other particles are excluded from this small habitat.

$$\begin{cases} d_i = \min\limits_{j \neq i}\left(\left\|X_i - X_j\right\|\right) \\ \sigma_{share} = \begin{cases} c & m < 2 \\ \sum\limits_{i=1}^{m} \dfrac{d_i}{m} & others \end{cases} \\ i, j = 1, 2, \cdots, m \end{cases} \tag{30}$$

where m is the number of particles contained in the population; c is an initial value constant (usually set to 1).

The iterative equations for the speed and position of the algorithm are as follows:

$$V_i^{k+1} = wV_i^k + c_1 rand_1\left(P_{best} - X_i^k\right) + c_2 rand_2\left(G_{best} - X_i^k\right) \tag{31}$$

$$X_i^{k+1} = X_i^k + V_i^{k+1} \tag{32}$$

where V_i^k is the velocity and direction of the kth search of the ith particle; X_i^k is the position of the kth search of the ith particle; w is the inertia weight; P_{best} is the individual optimal solution; G_{best} is the population optimal solution; c_1 and c_2 are the ability to make the particle have self-summary and learn from the best individuals in the population, respectively, which are the learning factors; $rand_1$ and $rand_2$ are a uniformly distributed random number between 0 and 1.

Moreover, the particle swarm algorithm based on the small habitat technology generally adopts a linear inertia weight decreasing strategy, which is a single adjustment method that cannot take good care of the global and local optimization seeking ability of the algorithm. Therefore, this paper proposes a nonlinear inertia weight decreasing strategy combining Gaussian distribution function, which is

$$w = w_{start} - \frac{w_{start} - w_{end}}{\sigma\sqrt{2\pi}} e^{-\frac{\left(\frac{t}{t_{max}} - \mu\right)^2}{2\sigma^2}} \tag{33}$$

where w_{start} is the initial value of inertia weight; w_{end} is the termination value of inertia weight; t is the number of current iterations; t_{max} is the maximum number of iterations; σ and μ are the adjustment coefficients of Gaussian distribution function. When $\mu = 0, \sigma = 1/\sqrt{2\pi}$ and $t = 0$, it is the initial weight. When $\mu = 0$, with the increasing number of iterations t, different descent effects can be obtained for different values of σ. When σ is small, the faster w will approach the weight termination value during the search, making the algorithm fall into local search; when σ is large, w takes a larger value at the beginning of the search, while w decreases nonlinearly as the number of iterations increases, making the algorithm have a stronger global search capability at the early stage and a stronger local search capability at the late iteration, speeding up the convergence speed.

The improved small-habitat particle swarm algorithm applied to integrated energy system scheduling optimization proceeds as follows:

Step 1: Set up the parameters and data of the integrated energy optimization model;
Step 2: Initialize each parameter of the algorithm and the particle population;
Step 3: Calculation of microhabitat radius and hence microhabitat grouping;
Step 4: Calculation of individual particle fitness, individual optimum and population optimum for small habitats;
Step 5: Update the velocity and position of particles;
Step 6: Updating particle individual fitness, small habitat individual optimality and population optimality;
Step 7: Continuous iteration using small habitat technology;
Step 8: Determine whether the maximum number of iterations is reached, and if it is satisfied, output the optimal individual, otherwise go to step 3 until the termination condition is satisfied;

5 CASE STUDIES

In this paper, a modified 6-bus power system with a 7-node natural gas system (He et al., 2016) and a modified 39-bus power

RETRACTED

TABLE 1 | Unit combinations for each time period in Cases 1–4.

Unit	Hours 1–24																							
	1	2	3	4	5	6	7	8	9	10	11	12	13	14	15	16	17	18	19	20	21	22	23	24
(A) Unit combinations for each time period in Cases 1–3																								
G1	1	1	1	1	1	1	**1**	**1**	**1**	1	1	**0**	**0**	**0**	1	1	1	1	1	1	1	1	0	0
G2	0	0	0	0	0	0	0	0	**0**	0	0	**1**	**1**	**1**	0	0	0	0	0	0	0	0	0	0
G3	1	1	0	0	0	0	**0**	**0**	**0**	1	1	1	1	1	1	1	1	1	1	1	1	1	1	1
G4	1	1	1	0	0	0	0	1	1	1	1	1	1	1	1	1	1	1	1	1	1	1	1	1
G5	1	1	1	1	1	1	1	1	1	1	1	1	1	1	1	1	1	1	1	1	1	1	1	1
(B) Unit combinations by time period in Case 4																								
G1	1	1	1	1	1	1	**0**	**0**	**0**	1	1	**1**	**1**	**1**	1	1	1	1	1	1	1	1	0	0
G2	0	0	0	0	0	0	0	0	**1**	0	0	**0**	**0**	**0**	0	0	0	0	0	0	0	0	0	0
G3	1	1	0	0	0	0	**1**	**1**	**1**	1	1	1	1	1	1	1	1	1	1	1	1	1	1	1
G4	1	1	1	0	0	0	0	1	1	1	1	1	1	1	1	1	1	1	1	1	1	1	1	1
G5	1	1	1	1	1	1	1	1	1	1	1	1	1	1	1	1	1	1	1	1	1	1	1	1

system (Zimmerman et al., 2011) with a 20-node natural gas system (Munoz et al., 2003) are used as examples of calculations to verify the effectiveness of the proposed model through simulation analysis. The scheduling period of the example is 24 h, and the length of a single period is 1 h.

5.1 6-Bus Electrical System With 7-Node Natural Gas System

The 6-bus electrical system and the 7-node natural gas system are shown in **Supplementary Appendix Figure SB1**. The 6-bus power system includes 2 gas-fired units G1-G2, 3 coal-fired units G3-G5, a wind farm, a photovoltaic power plant, an energy storage battery, an P2G facility, 7 transmission lines and 3 electric loads EL1-EL3. The coal-fired unit with the highest CO_2 emission intensity, G5, was converted to a carbon capture unit, which was installed on the power bus 3 along with the P2G facility. The 7-node gas system includes 2 gas wells GW1-GW2, 1 compressor, 1 storage facility, 6 gas pipelines and 3 gas loads GL1-GL3. Gas units G1-G2 are supplied by natural gas node 3 and natural gas node 1, respectively, and the methane synthesized by the P2G facility is injected into natural gas node 1.

The standby capacity of the power system at each time is set at 10% of the total load. The fixed energy consumption of the carbon capture system is 0.5% of the installed capacity of the unit, and the carbon tax price and the unit CO_2 transmission and storage price are set to 20$/t (Ji et al., 2013) and 200$/t (Ebaid et al., 2015), respectively. the maximum and minimum injection power of the P2G facility is 100 and 10 MW, respectively, and the capacity of the hydrogen storage equipment matches the maximum injection power of the P2G facility, and the maximum and minimum output power of the gas turbine is 20 and 2 MW, respectively. Other parameters such as the machine set are given in the literature (He et al., 2016), literature (Ban et al., 2017) and literature (He, 2020). The predicted values of wind power and photovoltaic power generation are shown in **Supplementary Appendix Figure SA1**, and the predicted values of electric load and gas load are shown in **Supplementary Appendix Figure SA2**.

To verify the validity of the proposed model, each of the four cases was set up as follows:

Case 1. Economic dispatch of integrated energy system without considering carbon capture system and P2G facility.

Case 2. Economic dispatch of integrated energy system with additional P2G facility based on Case 1.

Case 3. Economic dispatch of integrated energy system with carbon capture system based on Case 1.

Case 4. Economic dispatch of integrated energy system considering both carbon capture system and P2G facility.

It is worth stating that Case 1 is similar to the existing study (Alabdulwahab et al., 2017) and serves as a benchmark case.

5.1.1 Power System Unit Combination Results and Analysis

Table 1 lists the unit combination of Cases 1–4 in each period It can be seen that the combination of units is the same for each time period in Cases 1–3. After considering both the carbon capture system and the P2G facility, the start/stop situation of units G1-G3 in Case 4 will be different from that of Cases 1–3 in periods 7–9 and 12–14. This indicates that the simultaneous consideration of carbon capture systems and P2G facility has an impact on the economic dispatch of integrated energy systems.

5.1.2 Optimization Results and Analysis

The optimization results of Cases 1–4 are shown in **Figure 5**. In Cases 1–4, the optimization results for each case yield 30 Pareto optimal solutions, i.e., there are 30 control strategies available to the user for each case, and the operating and environmental costs for each control strategy vary.

The optimization results show that there is a constraint relationship between the two objectives, which cannot be optimized simultaneously. Under the consideration of economic benefits, the operating cost in the control strategy

RETRACTED

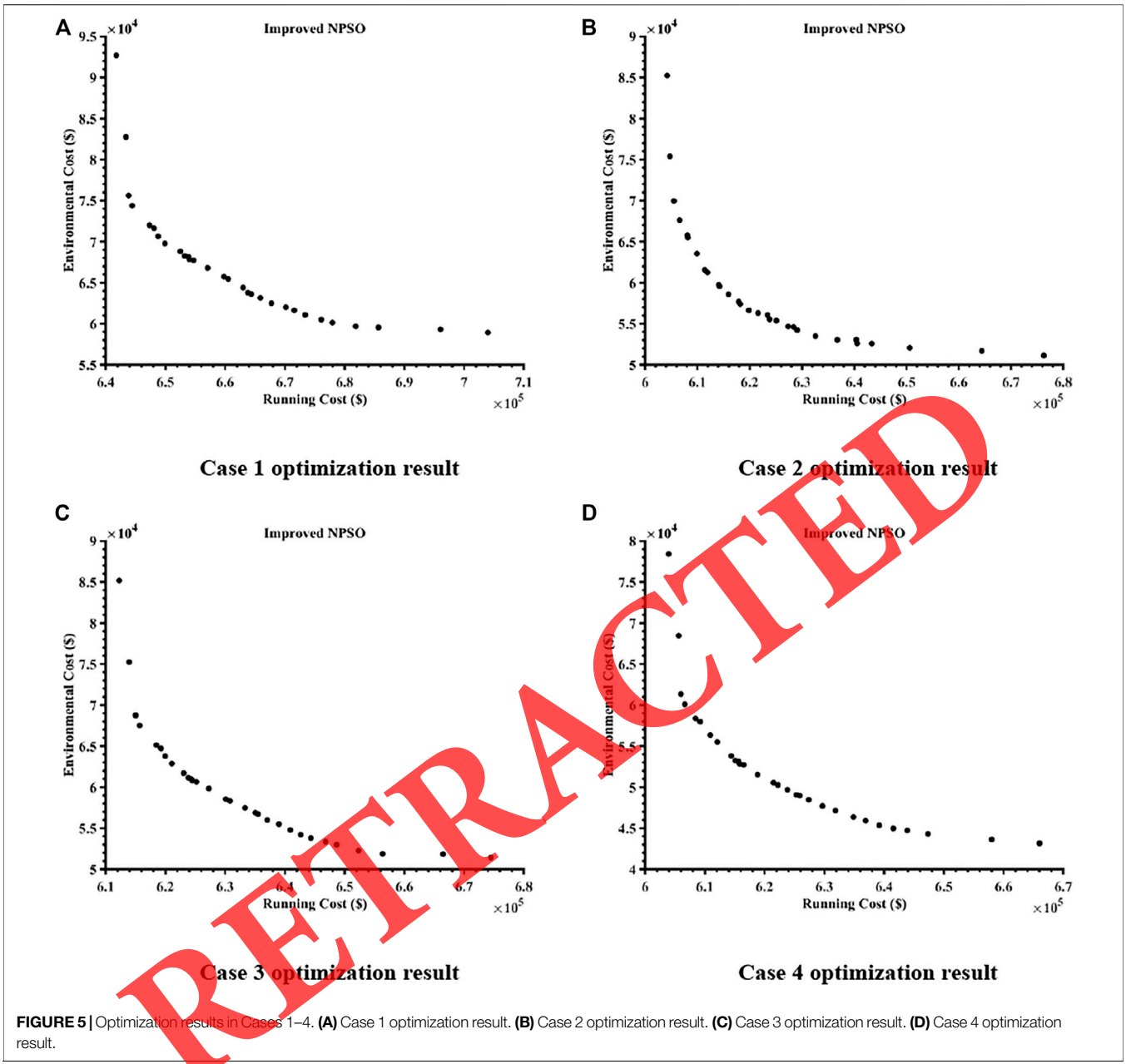

RETRACTED

FIGURE 5 | Optimization results in Cases 1–4. **(A)** Case 1 optimization result. **(B)** Case 2 optimization result. **(C)** Case 3 optimization result. **(D)** Case 4 optimization result.

TABLE 2 | Cost of the objective function in Cases 1–4.

Case	Total cost/$	Operation cost/$	Environmental cost/$
1	734,429.65	641,742.26	92,687.39
2	689,453.45	604,224.24	85,229.21
3	697,442.53	612,246.39	85,196.14
4	684,366.92	602,827.29	81,539.63

represented by any one Pareto optimal solution is much larger than the environmental cost, and thus the Pareto optimal solution with the lowest operating cost has excellent economic benefits, so the Pareto optimal solution with the lowest operating cost in the solution set of the above four cases is selected as the ideal solution and compared for analysis.

The costs of the objective functions in Cases 1–4 are shown in **Table 2**. It can be seen that the total cost, operation cost and environmental cost of Case 4 are optimal compared with Cases 1–3, which verifies the superiority of improving the economic dispatch of the integrated energy system by considering both the carbon capture system and the P2G facility. The methane synthesized by the P2G facility can reduce the natural gas supply to the gas wells and gas storage facilities, while the operation of the carbon capture system will bring the corresponding fixed and operational energy consumption, so the operating costs of Cases 2–4 are Case 3, Case 2, and Case

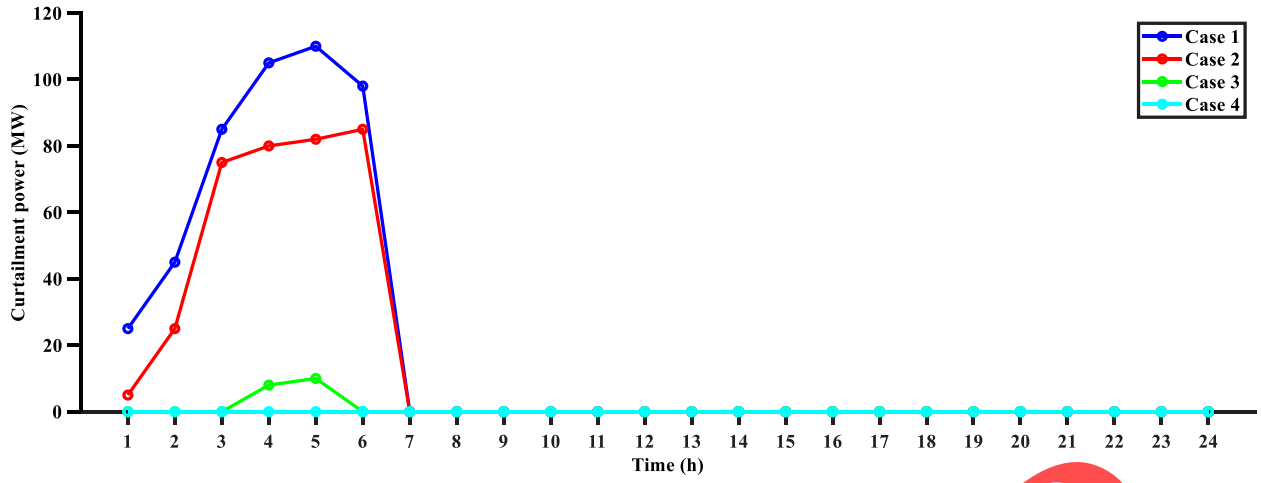

FIGURE 6 | Curtailment of wind and solar energy by time period.

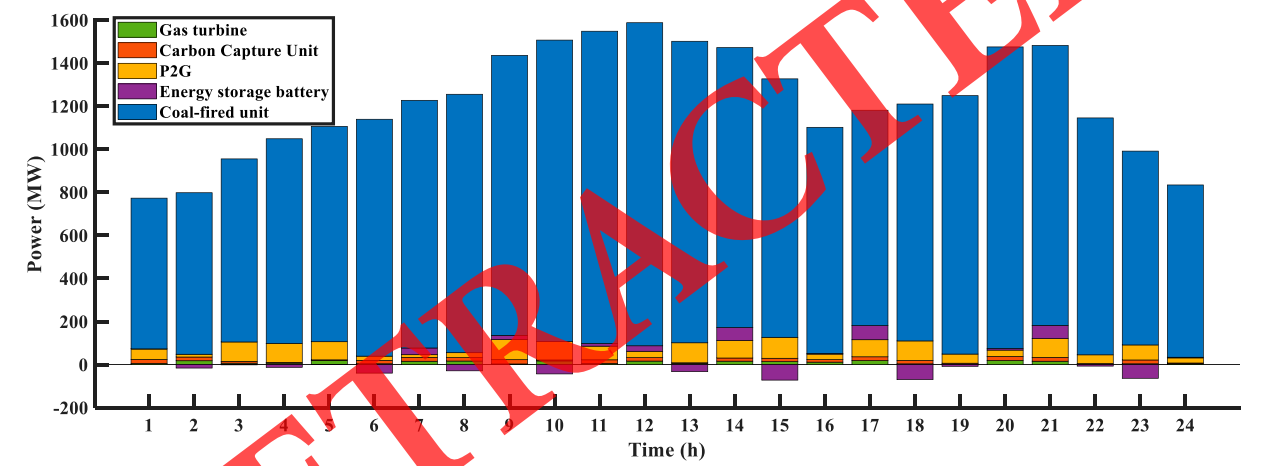

FIGURE 7 | Power load balance.

RETRACTED

4 in descending order. However, the corresponding carbon tax costs are lower than those of Cases 1–2, so the environmental costs of Cases 1–4 are, in descending order, Case 1, Case 2, Case 3, and Case 4.

The curtailment of wind and solar energy for each time period in Cases 1–4 is shown in **Figure 6**. It can be seen that in Case 1, wind and solar energy curtailment occurs in time periods 1–7. With the addition of carbon capture systems or P2G facility, Cases 2–3 can reduce the wind and solar energy curtailment. However, the operational energy consumption of the carbon capture system is limited by the amount of carbon dioxide captured, and the injection power of the P2G facility cannot exceed its capacity of 100 MW, so only one of the two can still not accommodate all the wind and solar energy. In Case 4, since both the carbon capture system and the P2G facility contribute to the wind and solar energy accommodation, the wind and solar energy can be fully utilized.

As a result of the above analysis, Case 4 has had a good impact on improving the economic dispatch of the integrated energy system. **Figure 7** shows the power load balance on the basis of Case 4. The electric power shown in the figure does not include the output of the wind turbine and PV as well as the electric load; the electric power of all three of them is calculated according to the predicted values in the previous section. In the grid part, the electrical load is carried by wind, solar, storage batteries, coal-fired units and gas turbines, where positive storage battery power means discharging and negative means charging.

Figure 8 shows the gas equilibrium on the basis of Case 4. It should be noted that the gas balance here refers to the hydrogen balance. The hydrogen produced by the P2G facility is partly stored in the hydrogen storage tank and partly used in the Sabatier reaction to produce methane. The generated methane is partly injected into the natural gas network and partly supplied to the gas turbine,

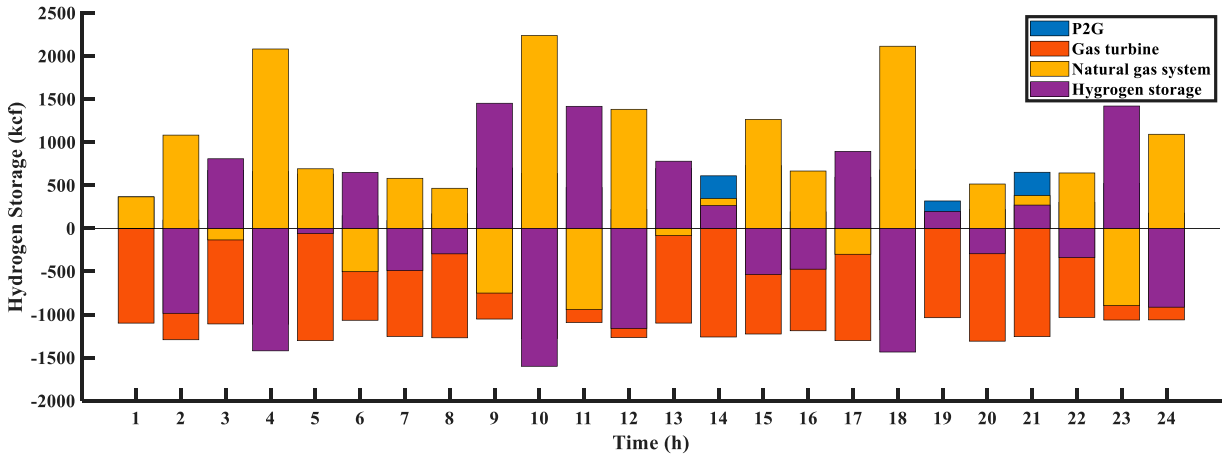

FIGURE 8 | Gas balance.

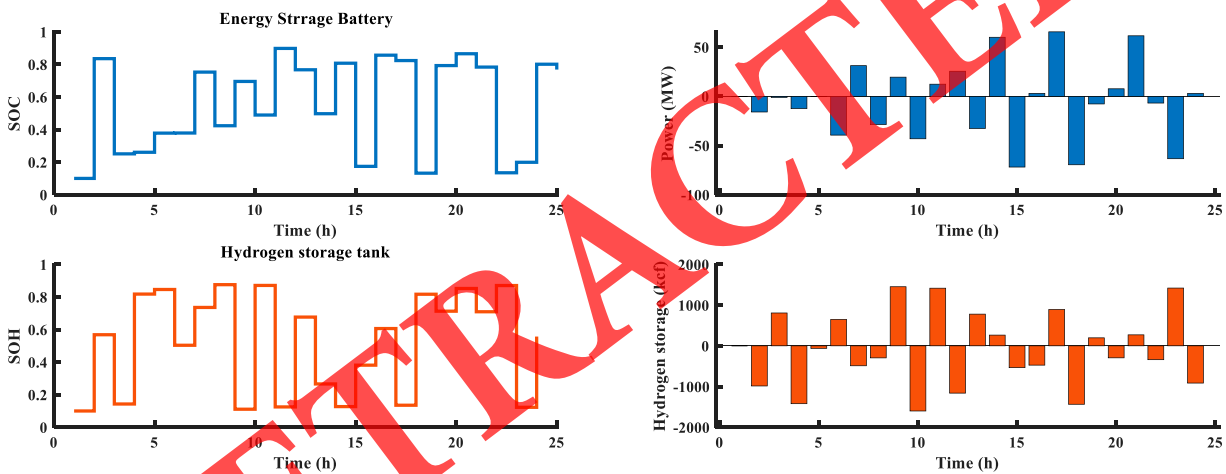

FIGURE 9 | The working of energy storage battery and hydrogen storage tank.

RETRACTED

which means that the gas turbine and the natural gas network will indirectly consume the hydrogen produced by the P2G facility.

Figure 9 shows the operation of the energy storage cell and the hydrogen storage tank on the basis of Case 4 for the whole dispatch cycle. It should be noted that the SOH, i.e. the ratio of the current hydrogen storage capacity of the hydrogen storage tank to its nominal capacity, is used here to indicate the current state of the hydrogen storage tank. Where, a positive storage battery power means discharging and a negative one means charging; a positive hydrogen storage volume of the hydrogen storage tank means injecting hydrogen and a negative one means releasing hydrogen. The presence of the hydrogen storage equipment allows the gas network to work with the carbon capture system to synthesize methane via the Sabatier reaction during times of high natural gas demand, providing a degree of "peak shaving" to the natural gas network.

Figure 10 shows the carbon dioxide emission and carbon capture treatment based on Case 4. Here, the CO_2 emission is mainly considered by the CO_2 emitted from the coal-fired unit, and the captured CO_2 is mainly considered by the CO_2 captured by the carbon capture system, and the two are considered together to get the equivalent emission CO_2 curve.

Figure 11 shows the synthesis of methane from the P2G facility based on Case 4. The hydrogen produced by the P2G facility synthesizes methane with the carbon dioxide captured by the carbon capture system, and the presence of the carbon and hydrogen storage plants enables the decoupling of the electro-hydrogen and hydrogen methanation processes in time to a certain extent, so that the methane can be synthesized during the periods 8, 11, and 23 when the natural gas demand is high.

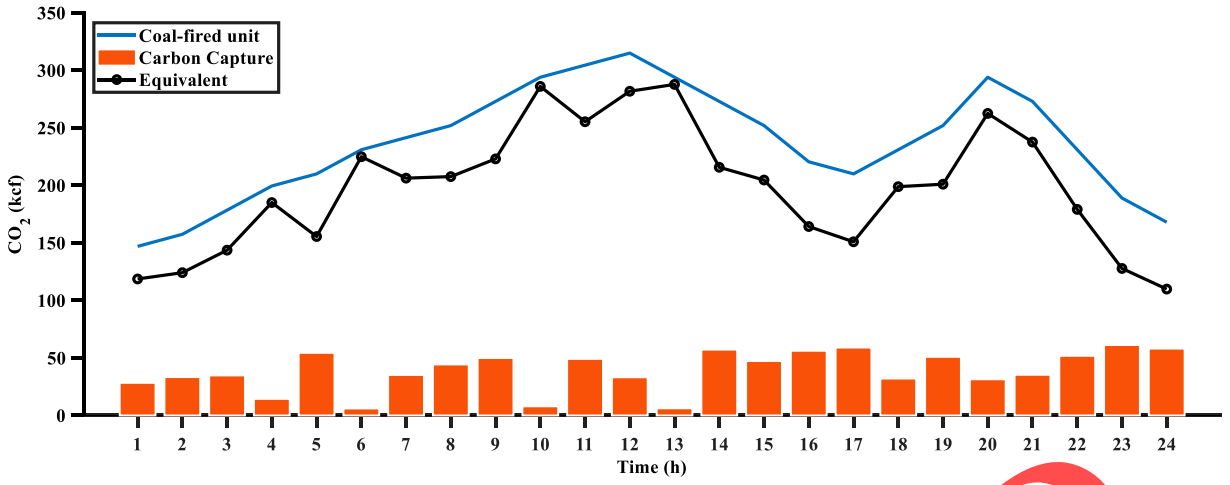

FIGURE 10 | Carbon dioxide emissions and carbon capture treatment.

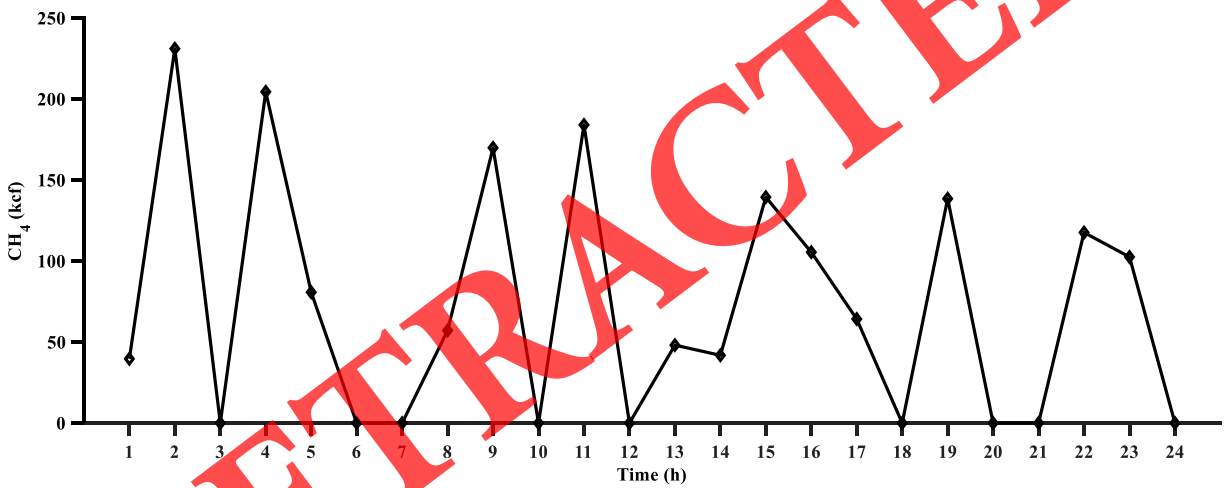

FIGURE 11 | Synthetic methane.

RETRACTED

TABLE 3 | Cost of the objective function in Cases 1–4.

Case	Total cost/$	Operation cost/$	Environmental cost/$
1	23,224,076.21	20,964,835.35	2,259,240.86
2	20,969,774.03	19,865,350.74	1,104,423.29
3	21,121,013.24	20,112,046.73	1,008,966.51
4	20,799,835.94	19,798,549.96	1,001,285.98

5.2 39-Bus Electric System With 20-Node Natural Gas System

In order to analyze the simulation of Cases 1–4 in the above small example under a larger integrated energy system, a modified 39-bus electric system and a 20-node natural gas system are presented in **Supplementary Appendix Figure SB2**. G1, G7, and G8 in the power system are gas-fired units, which get natural gas from nodes 5, 14, and 2 of the natural gas system, respectively, while the other fossil fuel units are coal-fired units. Coal-fired units G9 and G10 are converted to carbon capture units, which are connected to bus 38 and bus 39 of the power system with P2G facility P2G1 and P2G2, respectively. Meanwhile, wind farms with capacities of 700 and 900 MW and photovoltaic farms with capacities of 700 and 800 MW are installed in power bus 32 and power bus 33, respectively, and energy storage batteries with a total capacity of 450 MW are installed in power node 35. Methane synthesized by the P2G facility P2G1 and P2G2 is injected into the natural gas pipeline through natural gas system nodes 8 and 14. Other parameters such as the machine set are given in the literature (Zimmerman et al., 2011), literature (Munoz et al., 2003) and literature (He, 2020).

The costs of the objective functions in Cases 1–4 are shown in **Table 3**. Similar to the simulation results in 5.1, the total cost, operating cost and environmental cost of Case 4 are optimal

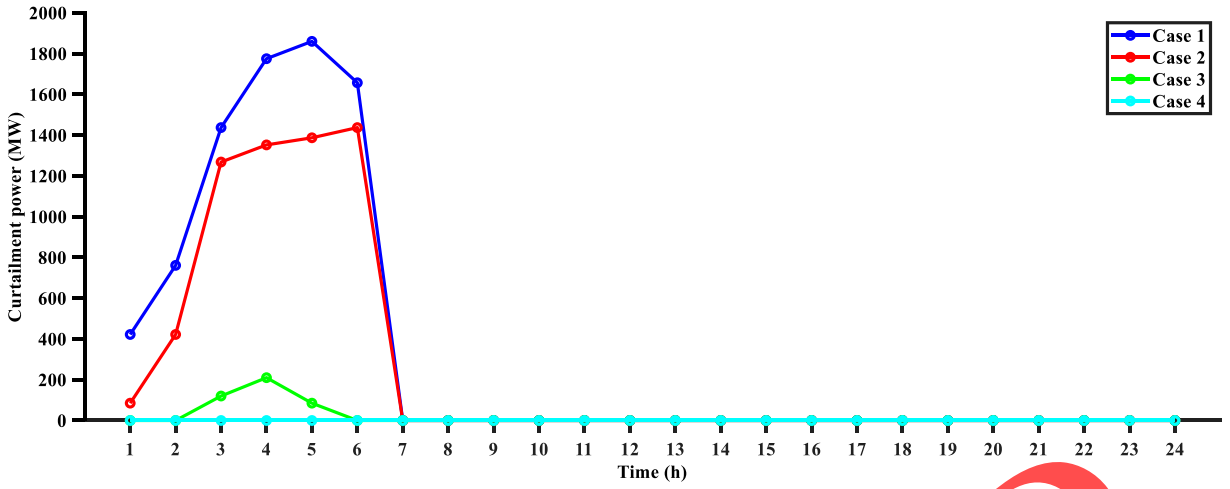

FIGURE 12 | Curtailment of wind and solar energy by time period.

compared with Cases 1–3, which verifies the superiority of improving the economic dispatch of the integrated energy system by considering both the carbon capture system and the P2G facility.

The curtailment of wind and solar energy for each time period in Cases 1–4 is shown in **Figure 12**. Similar to the simulation results in 5.1, the economic dispatch of the integrated energy system in Case 1 has a large curtailment of wind and solar energy. Cases 2–3 are equipped with P2G facility and carbon capture system respectively, which can improve the curtailment of wind and solar energy better. In Case 4, both P2G facility and carbon capture system are installed, and the surplus wind and solar energy can be fully accommodated.

6 CONCLUSION

In order to improve the economy of the integrated energy system and the capacity of wind and solar energy accommodation, a bi-level optimal dispatch model of the integrated energy system is developed in this paper, taking into account the carbon capture system and the P2G facility. The upper model is the optimal allocation model for coal-fired units, and the lower model is the economic dispatch model for the integrated energy system, and the upper model is solved by converting the model into a mixed-integer linear programming problem and calling CPLEX, while the lower model is a multi-objective planning problem, and the model is solved by improving the small-habitat particle swarm algorithm. The conclusions obtained from the algorithm analysis are as follows:

(1) The total cost, operation cost and environmental cost of the integrated energy system economic dispatch considering both the carbon capture system and the P2G facility are optimal. Among them, the total cost of economic dispatch of integrated energy system is reduced by about 6.82%, the operating cost of economic dispatch of integrated energy system is reduced by about 6.06%, and the environmental cost of economic dispatch of integrated energy system is reduced by about 12.03%.

(2) Adding P2G facility and carbon capture systems can reduce wind and solar energy curtailment by 22.73 and 90.91%, respectively, while adding both P2G facility and carbon capture systems can accommodate all the surplus wind and solar energy.

(3) In the subsequent research work, the joint optimization scheme of demand-side standby resources with flexible and fast dispatching carbon capture power plant standby resources at different time scales and other related studies will be considered.

DATA AVAILABILITY STATEMENT

The original contributions presented in the study are included in the article/**Supplementary Material**, further inquiries can be directed to the corresponding author.

AUTHOR CONTRIBUTIONS

All authors listed have made a substantial, direct, and intellectual contribution to the work and approved it for publication.

FUNDING

This work is financially supported by the Postgraduate Research and Practice Innovation Program of Jiangsu Province (No. SJCX21_1777).

SUPPLEMENTARY MATERIAL

The Supplementary Material for this article can be found online at: https://www.frontiersin.org/articles/10.3389/fenrg.2021.784703/full#supplementary-material

RETRACTED

REFERENCES

Alabdulwahab, A., Abusorrah, A., Zhang, X., and Shahidehpour, M. (2017). Coordination of Interdependent Natural Gas and Electricity Infrastructures for Firming the Variability of Wind Energy in Stochastic Day-Ahead Scheduling[J]. *IEEE Trans. Sust. Energ.* 6 (2), 606–615. doi:10.1109/tste.2015.2399855

Bai, L., Li, F., Cui, H., Jiang, T., Sun, H., and Zhu, J. (2016). Interval Optimization Based Operating Strategy for Gas-Electricity Integrated Energy Systems Considering Demand Response and Wind Uncertainty. *Appl. Energ.* 167, 270–279. doi:10.1016/j.apenergy.2015.10.119

Bai, L., Li, F., Cui, H., Jiang, T., Sun, H., and Zhu, J. (2016). Interval Optimization Based Operating Strategy for Gas-Electricity Integrated Energy Systems Considering Demand Response and Wind Uncertainty. *Appl. Energ.* 167, 270–279. doi:10.1016/j.apenergy.2015.10.119

Ban, M., Yu, J., Shahidehpour, M., and Yao, Y. (2017). Integration of Power-To-Hydrogen in Day-Ahead Security-Constrained Unit Commitment with High Wind Penetration. *J. Mod. Power Syst. Clean. Energ.* 5 (3), 337–349. doi:10.1007/s40565-017-0277-0

Barry, Azzopardi., and Menon, E. Shashi. (2005). *Gas Pipeline Hydraulics*. Boca Raton, FL: CRC Press/Taylor & Francis Group. 0849327857, £74.99/$129.95.[J]. Fuel.

Chang, Jinwei., Li, Zhi., Huang, Yan., Yu, Xiaonan., Jiang, Ruicheng., Huang, Rui., et al. (2021). Multi-objective Optimization of a Novel Combined Cooling, Dehumidification and Power System Using Improved M-PSO Algorithm. *Energy* 239, 122487. doi:10.1016/j.energy.2021.122487

Chen, Qixin., Kang, Chongqing., and Xia, Qing. (2010). Operation Mechanism and Peak-Load Shaving Effects of Carbon-Capture Power Plant[J]. *Proc. CSEE* 30 (7), 22–28. doi:10.13334/j.0258-8013.pcsee.2010.07.004

Chen, Qixin., Zhen, J. I., Kang, Chongqing., and Hao, M. (2012). Analysis on Relation between Power Generation and Carbon Emission of Carbon Capture Power Plant in Different Operation Modes[J]. *Automation Electric Power Syst.* 36 (18), 109–115. doi:10.3969/j.issn.1000-1026.2012.18.020

Clegg, S., and Mancarella, P. (2015). Integrated Modeling and Assessment of the Operational Impact of Power-To-Gas (P2G) on Electrical and Gas Transmission Networks. *IEEE Trans. Sustain. Energ.* 6 (4), 1234–1244. doi:10.1109/tste.2015.2424885

Correa-Posada, C. M., and Sanchez-Martin, P. (2014). Security-Constrained Optimal Power and Natural-Gas Flow. *IEEE Trans. Power Syst.* 29 (4), 1780–1787. doi:10.1109/tpwrs.2014.2299714

Cui, H., Li, F., Hu, Q., Bai, L., and Fang, X. (2016). Day-ahead Coordinated Operation of Utility-Scale Electricity and Natural Gas Networks Considering Demand Response Based Virtual Power Plants. *Appl. Energ.* 176, 183–195. doi:10.1016/j.apenergy.2016.05.007

Cui, Yang., Deng, Guibo., Zeng, Peng., Zhong, Wuzhi., Zhao, Yuting., and Liu, Xinyuan. (2021a). Multi-Time Scale Source-Load Dispatch Method of Power System with Wind Power Considering Low-Carbon Characteristics of Carbon Capture Power Plant[J/OL]. *Proc. CSEE*, 1–18. 09-25. doi:10.13334/j.0258-8013.pcsee.210697

Cui, Yang., Deng, Guibo., Zhao, Yuting., Zhong, Wuzhi., Tang, Yaohua., and Liu, Xinyuan. (2021b). Economic Dispatch of Power System with Wind Power Considering the Complementarity of Low-Carbon Characteristics of Source Side and Load Side[J]. *Proc. CSEE* 41 (14), 4799–4815. doi:10.13334/j.0258-8013.pcsee.202533

Cui, Yang., Yan, S., and Zhong, W. (2020). Optimal Thermoelectric Dispatching of Regional Integrated Energy System with power-to-Gas[J]. *Power Syst. Tech.* 44 (11), 4254–4263. doi:10.13335/j.1000-3673.pst.2019.2468

Cui, Yang., Zeng, Peng., and Hui, Xinxin. (2021c). Low-carbon Economic Dispatch Considering the Integrated Flexible Operation Mode of Carbon Capture Power Plant[J]. *Power Syst. Tech.* 45 (05), 1877–1886. doi:10.13335/j.1000-3673.pst.2020.0404

Du, Xiabing., Yang, Xiaodong., Wang, Jiayao., Wang, Guofeng., and Zhang, Youbing. (2017). "Coordinated Optimal Control Strategy for Multi-Energy Microgrids Considering P2G Technology and Demand Response," in IEEE Conference on Energy Internet and Energy System Integration, Beijing, November 26–28, 2017, 1–6. doi:10.1109/EI2.2017.8245337

Ebaid, M. S. Y., Hammad, M., and Alghamdi, T. (2015). THERMO Economic Analysis of PV and Hydrogen Gas Turbine Hybrid Power Plant of 100 MW Power Output. *Int. J. Hydrogen Energ.* 40 (36), 12120–12143. doi:10.1016/j.ijhydene.2015.07.077

Ebel, R. E., Croissant, M. P., Masih, J. R., Calder, K. E., and Thomas, R. G. G. (1996). International Energy Outlook: U.S. Department of Energy. *Wash. Q.* 19 (4), 70–99. doi:10.1080/01636609609550217

Götz, M., Lefebvreb, J., Mörsa, F., Koch, A. M., Graf, F., and Bajohr, S., (2016). Renewable Power- to- Gas: A Technological and Economic Review[J]. *Renew. Energ.* 85, 1371–1390. doi:10.1016/j.renene.2015.07.066

Guandalini, G., Campanari, S., and Romano, M. C. (2015). Romano. Power-To-Gas Plants and Gas Turbines for Improved Wind Energy Dispatchability: Energy and Economic Assessment. *Appl. Energ.* 147, 117–130. doi:10.1016/j.apenergy.2015.02.055

He, C., Lei, W., Liu, T., and Shahidehpour, S. (2016). Robust Co-optimization Scheduling of Electricity and Natural Gas Systems via ADMM[J]. *IEEE Trans. Sust. Energ.* (99), 658–670. doi:10.1109/TSTE.2016.2615104

He, Liangce. (2020). *Research on Environmental Economic Dispatch of Integrated Electricity and Natural Gas system[D]*. Qinhuangdao: Yanshan University.

He, L., Lu, Z., Lu, J., Geng, L., Zhao, H., and Li, X. (2018). Low-carbon Economic Dispatch for Electricity and Natural Gas Systems Considering Carbon Capture Systems and Power-To-Gas. *Appl. Energ.* 224, 357–370. doi:10.1016/j.apenergy.2018.04.119

Hu, Diangang., Pan, Zhengjie., Xu, Haoliang., and Jin, P. (2017). Peaking Capacity Estimation of Natural Gas Unit under the Condition of Large-Scale Renewable Energy Connecting with Power Grid[J]. *Power Syst. Prot. Control.* 45 (3), 87–93. doi:10.7667/PSPC160188

Ji, Z., Kang, C., Chen, Q., Xia, Q., Jiang, C., Chen, Z., et al. (2013). Low-Carbon Power System Dispatch Incorporating Carbon Capture Power Plants. *IEEE Trans. Power Syst.* 28 (4), 4615–4623. doi:10.1109/tpwrs.2013.2274176

Kang, Chongqing., Zhen, J. I., and Chen, Qixin. (2012). Review and Prospects of Flexible Operation of Carbon Capture Power Plants[J]. *Automation Electric Power Syst.* 36 (6), 1–10. doi:10.7500/AEPS201202121

Kennedy, J., and Eberhart, R. (1995). "Particle Swarm Optimization," in Proceedings of ICNN'95 - International Conference on Neural Networks, Perth, WA, November 27–December 1, 1995, 1942–1948.4. doi:10.1109/icnn.1995.488968

Li, G., Zhang, R., Jiang, T., Chen, H., Bai, L., Cui, H., et al. (2017). Optimal Dispatch Strategy for Integrated Energy Systems with CCHP and Wind Power. *Appl. Energ.* 192, 408–419. doi:10.1016/j.apenergy.2016.08.139

Lin, D. U., Sun, Liang., and Chen, Houhe. (2017). Multi-index Evaluation of Integrated Energy System with P2G Planning[J]. *Electric Power Automation Equipment* 37 (6), 110–116. doi:10.16081/j.issn.1006-6047.2017.06.015

Lin, Kaidong., Chen, Zexing., and Zhang, Yongjun. (2019). Wind Power Accommodation and Successive Linear Low-Carbon Economic Dispatch of Integrated Electricity-Gas Network with Power to Gas[J]. *Automation Electric Power Syst.* 43 (21), 23–33. doi:10.7500/AEPS20190411004

Liu, J., Sun, W., and Yan, J. (2021). Effect of P2G on Flexibility in Integrated Power-Natural Gas-Heating Energy Systems with Gas Storage. *Energies* 14 (1), 196. doi:10.3390/en14010196

Lu, K., and Li, Y. Y. (2019). A Robust Locating Multi-Optima Approach for Damage Identification of Plate-like Structures. *Appl. Soft Comput.* 75, 508–522. ISSN 1568-4946. doi:10.1016/j.asoc.2018.11.035

Lu, S., Lou, S., Wu, Y., and Yin, X (2013) Power System Economic Dispatch under Low-Carbon Economy with Carbon Capture Plants Considered[J]. *IET Generation* 7(9):991-1001. doi:10.1049/iet-gtd.2012.0590

Munoz, J., Jimenez-Redondo, N., Perez-Ruiz, J., and Barquin, J. (2003). "Natural Gas Network Modeling for Power Systems Reliability Studies," in 2003 IEEE Bologna Power Tech Conference Proceedings, Bologna, Italy, June 23–26, 2003 4, 20–27. doi:10.1109/PTC.2003.1304696

Qadir, A., Sharma, M., Parvareh, F., Khalilpour, R., and Abbas, A. (2015). Flexible Dynamic Operation of Soalr- Integrated Power Plant with Solvent Based post-combustion Carbon Capture(PCC) Process[J]. *Energ. Convers. Manag.* 97, 7–19. doi:10.1016/j.enconman.2015.02.074

RETRACTED

Rani, P., and Mahapatra, G. S. (2019). A Novel Approach of NPSO on Dynamic Weighted NHPP Model for Software Reliability Analysis with Additional Fault Introduction Parameter. *Heliyon* 5 (Issue 7), e02082. doi:10.1016/j.heliyon.2019.e02082

Sun, Guoqiang., sheng, Chen., Zheng, Yuping., and Wei, Z. (2015). Available Transfer Capability Calculation Considering Electricity and Natural Gas Coupled Energy System Security Constrains[J]. *Automation Electric Power Syst.* 39 (23), 26–32. doi:10.7500/AEPS20150625006

Tan, R. R., Sum Ng, D. K., and Yee Foo, D. C. (2009). Pinch Analysis Approach to Carbon-Constrained Planningfor Sustainable Power Generation. *J. Clean. Prod.* 17, 940–944. doi:10.1016/j.jclepro.2009.02.007

Tomasgard, A., Rmo, F., Fodstad, M., and Midthun, K. (2007). *Optimization Models for the Natural Gas Value Chain[M]*. Springer Berlin Heidelberg.

Wei, Zhinong., Zhang, Side., Sun, Guoqiang., and Zhang, H. (2017). Power-to-gas Considered Peak Load Shifting Research for Integrated Electricity and Natural-Gas Energy Systems[J]. *Proc. CSEE* 37 (16), 4601–4609. doi:10.13334/j.0258-8013.pcsee.161361

Xu, Zizhi., and Zeng, Ming. (2011). Analysis on Electricity Market Development in US and its Inspiration to Electricity Market Construction in China[J]. *Power Syst. Tech.* 35 (6), 161–166. doi:10.13335/j.1000-3673.pst.2011.06.004

Yang, J., Zhang, N., Cheng, Y., Kang, C., and Xia, Q. (2018). Modeling the Operation Mechanism of Combined P2G and Gas-Fired Plant with CO2 Recycling[J]. *IEEE Trans. Smart Grid* 10 (1), 1111–1121. doi:10.1109/tsg.2018.2849619

Yang, L. I., Liu, Weijia., Zhao, Junhua., and Wen, F (2016). Optimal Dispatch of Combined Electricity-Gas-Heat Energy Systems with Power-To- Gas Devices and Benefit Analysis of Wind Power Accommoda- Tion[J]. *Power Syst. Tech.* 40 (12), 3680–3689. doi:10.13335/j.1000-3673.pst.2016.12.008

Yu, Juan., Ma, Mengnan., Guo, Lin., and Zhang, S. (2018). Reliability Evaluation of Integrated Electrical and Natural-Gas System with power-to-Gas[J]. *Proc. CSEE* 38 (3), 708–715. doi:10.13334/j.0258-8013.pcsee.170980

Yuan, P. E. N. G., Low, Suhua., and Wu, yaowu. (2021). Low-carbon Economic Dispatch of Power System with Wind Power Considering Solvent-Storaged Carbon Capture Power plant[J/OL]. *Trans. China Electrotechnical Soc.* 1-9. , 2021 06-01. doi:10.19595/j.cnki.1000-6753.tces.201249

Zhang, Chi., Tang, Qinghua., Yan, Wei., and Jufang, W. (2017). Reliability Evaluation of Integrated Community Energy System Based on Particle-Swarm- interior-point Hybrid Optimization Algorithm[J]. *Electric Power Construction* 38 (12), 104–111. doi:10.3969/j.issn.1000-7229.2017.12.013

Zhang, Rufeng., Jiang, Tao., and Guoqing, L. I. (2018a). Bi-level Optimization Dispatch of Integrated Electricity-Natural Gas Systems Considering P2G for Wind Power Accommodation[J]. *Proc. CSEE* 38 (19), 5668–5678. doi:10.13334/j.0258-8013.pcsee.172310

Zhang, X., Shahidehpour, M., Alabdulwahab, A., and Abusorrah, A. (2015). Hourly Electricity Demand Response in the Stochastic Day-Ahead Scheduling of Coordinated Electricity and Natural Gas Networks[J]. *IEEE Trans. Power Syst.* 31 (1), 592–601. doi:10.1109/TPWRS.2015.2390632

Zhang, Youbing., Wang, Jiayao., Yang, Xiaodong., and Du, X. (2018b). An Online Optimal Scheduling Approach for Regional Integrated Energy System Considering P2G[J]. *Power Syst. Tech.* 42 (8), 2467–2477. doi:10.13335/j.1000-3673.pst.2017.3040

Zimmerman, R. D., Murillo-Sanchez, C. E., and Thomas, R. J. (2011). MATPOWER: Steady-State Operations, Planning, and Analysis Tools for Power Systems Research and Education. *IEEE Trans. Power Syst.* 26 (1), 12–19. doi:10.1109/tpwrs.2010.2051168

Conflict of Interest: The authors declare that the research was conducted in the absence of any commercial or financial relationships that could be construed as a potential conflict of interest.

Publisher's Note: All claims expressed in this article are solely those of the authors and do not necessarily represent those of their affiliated organizations, or those of the publisher, the editors and the reviewers. Any product that may be evaluated in this article, or claim that may be made by its manufacturer, is not guaranteed or endorsed by the publisher.

Copyright © 2022 Zhang, Du, Li, Guo, Xu and Li. This is an open-access article distributed under the terms of the Creative Commons Attribution License (CC BY). The use, distribution or reproduction in other forums is permitted, provided the original author(s) and the copyright owner(s) are credited and that the original publication in this journal is cited, in accordance with accepted academic practice. No use, distribution or reproduction is permitted which does not comply with these terms.

RETRACTED